

Hierarchical design in the bimodal grains of ultrafine grain steel via ratio regulation on the dual-phase ferrite/martensite

Qingxiao Zhang¹, Xiaohua Wei^{1*}, Qing Yuan², Yunfeng Wang²

¹*School of Mechatronic Engineering, Quzhou College of Technology, Quzhou 324000, P. R. China*

²*State Key Laboratory of Refractories and Metallurgy, Wuhan University of Science and Technology, Wuhan 430081, P. R. China*

Received 17 October 2023, received in revised form 10 December 2024, accepted 14 February 2025

Abstract

Thermal holding at critical temperature to obtain ferrite and martensite dual-phase microstructure was adopted to fabricate the ultrafine ferrite grains with a bimodal distribution. Microstructure evolution and mechanical properties by different holding times were analyzed. Results showed that the hierarchical design in the bimodal grains of UFGs via ratio regulation on the dual-phase ferrite/martensite could be achieved by holding time. The tensile strength decreased with the increased holding time at critical temperature, while the elongation increased with the increase of holding time. The comprehensive mechanical properties were dominated by the volume fraction of introduced ferrite and the final grain size distribution. Furthermore, the elongation was ensured by the better work hardening ability in coarsening grains and plastic strain gradient between ferrite grains with a bimodal distribution.

Key words: ultrafine grain, bimodal grain, ferrite, martensite, tensile strength, ductility

1. Introduction

Ultrafine grain (UFG) steel, as a representative advanced high-performance structural material, achieves strengthening and toughening through grain ultrafining completely different from the traditional alloy element addition and heat treatment [1–3]. This method could fully tap the potential of materials and then obtain the best comprehensive performance. Therefore, ultrafine grain is considered to achieve comprehensive performance upgrading of the traditional steel materials [4, 5].

Many different methods were developed to achieve grain refinement in steels or other alloys, and severe plastic deformation (SPD) was the most promising method to obtain bulk UFGs with excellent mechanical properties. In recent years, a series of SPD processes such as Equal Channel Angular Pressing (ECAP) [6, 7], High-Pressure Torsion (HPT) [8, 9], and Accumulative Roll-Bonding (ARB) [10, 11] have been developed through the continuous efforts of researchers. The results indicated that the decrease in grain size tremendously led to the decrease of

work hardening capacity and uniform elongation in the UFGs while improving the material strength. Especially when the grain size reached submicron, the uniform elongation in UFGs decreased significantly, severely limiting its application as a structural material. The decrease in plasticity of ultrafine/nanocrystalline metals and alloys was mainly due to the failure of dislocation accumulation inside the small grain size and the deteriorating work hardening [12, 13].

The architecture of UFG materials, which combined coarse and fine grains, effectively overcame the shortcomings in ultrafine grain. In recent years, the gradient structure in metals has become a research topic [2, 14, 15]. The common gradient structure in metals was the size variation from micro/nanostructure on the surface to the relative coarse grains in the core, i.e., in the research of Lu et al. [16]. The surface mechanical attrition treatment was applied to obtain the nanocrystalline surface in 316L austenitic stainless steel with 1450 MPa yield strength. Results illustrated that the grain size could be refined to about 40 nm by surface severe plastic de-

*Corresponding author: e-mail address: 1456046192@qq.com

formation. In the investigation of Roland et al. [17], a gradient structure with 40 μm thickness in 316L austenitic stainless steel was obtained. It illustrated that the fatigue strength was improved in both low-cycle and high-cycle fatigue experiments in gradient 316L austenitic stainless steel. The increase in fatigue limit was due to the surface gradient nanostructure rather than the residual stress in the sample. However, most investigations about the gradient structure were widely reported in the Cu, Mg, and Al alloys [2, 14, 18], and relatively little literature about the gradient structure in steels could be found. Another gradient structure with micro/nanostructures in the core and coarse grains on the surface was also pointed out [19, 20]. However, the gradient structure in UFGs was hard to realize due to its complicated process, which was extremely difficult for industrial production.

To improve the plasticity of UFG materials and prevent the reduction of uniform elongation, it was necessary to compensate for the work hardening. It was clear that work hardening was difficult to occur in single-phase ultrafine materials. Therefore, bimodal grain size distribution with relatively large grain size mixed in the UFG matrix was proposed to establish a new architecture in UFG materials. H. Azizi-Alizamini et al. produced bimodal grain structures in low-carbon steels by cold rolling dual-phase structures and subsequent annealing. They claimed that these bimodal grain microstructures are interesting for optimizing the balance of strength and uniform elongation in UFGs [21]. A similar method was utilized and reported by T. S. Wang et al., and they demonstrated that there was a remarkable difference in carbon and alloy element content in the bimodal grain [22]. High-temperature, short-time annealing was applied to obtain bimodal grains in UFGs in the research of S. M. Hosseini et al. They reported that the observed excellent balance of ductility and strength was caused by the bimodal grain structures and contributed to the cementite within the coarse grains [23]. In the study of Yuan et al. [12], bimodal grains with an average size of 0.35 μm were developed by Nb addition in the low carbon steel, and the tensile strength reached about 990.8 MPa with 15.5% elongation. It illustrated that the not sharply decreased elongation was attributed to the enhanced work hardening by bimodal grains. Similar results were also exhibited in [13, 24]. In addition to the structural change in UFGs, the variation of second-phase particles was also considered to adjust the mechanical properties of UFGs. Nonetheless, the mechanical properties of UFGs were greatly sensitive to the distribution of second-phase particles, and then the relationship between strength and ductility was difficult to coordinate. Furthermore, the choice of second-phase particles was also complicated because of their different roles in UFGs.

Many reported works have evidenced the posi-

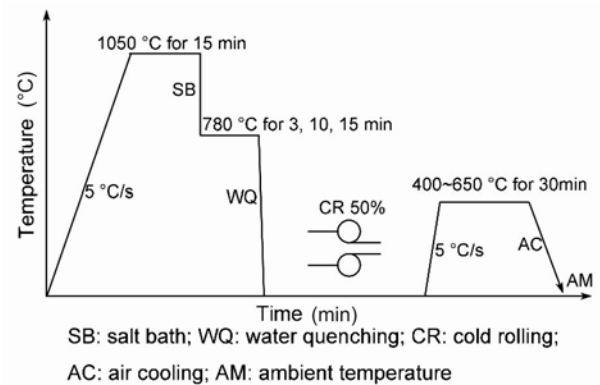


Fig. 1. Fabrication of bimodal grains in UFGs by critical temperature of 780 °C and different holding times.

tive effect of bimodal grain size distribution on the strength and ductility of UFGs, especially for industrial production. Meanwhile, the quantitative correlation between the mechanical properties and ratio of coarse-fine grains is neglected. The present study carried out a hierarchical design in the bimodal grains of UFGs via ratio regulation on the dual-phase ferrite/martensite. The time and temperature for obtaining bimodal grains were both considered. More data support was provided to design UFGs with desired mechanical properties accurately.

2. Materials and experimental methods

Q235 steel with a chemical composition of Fe-0.165 C-0.211 Si-0.448 Mn-0.014 P-0.013 S-0.002 Al (wt.%) was used as the experimental steel. Strip specimens were firstly re-austenitized at 1050 °C for 15 min, followed by the salt bath at 780 °C for 3, 10, and 15 min to obtain ferrite. Then, the specimens were quenched in room temperature water to realize the dual-phase microstructure of ferrite and martensite. Cold rolling by 50% reduction was carried out on a two-high mill with a roll diameter of 310 mm. Finally, the cold rolled dual-phase specimens were annealed at 400–650 °C for 30 min, and then air cooled to ambient temperature. In this experiment, one critical temperature of 780 °C was determined, and three different holding times to form different volume fractions of ferrite were designed. In addition, in-situ observation was conducted to clarify the ferrite transformation at the critical temperature of 780 °C.

ZEISS Optical microscope (OM) and Nova 400 Nano field emission scanning electron microscope (FE-SEM) were used to clarify the microstructure evolutions. Besides, the mechanical properties along the rolling direction were determined on an Instron-3382 electronic universal tensile testing machine with a

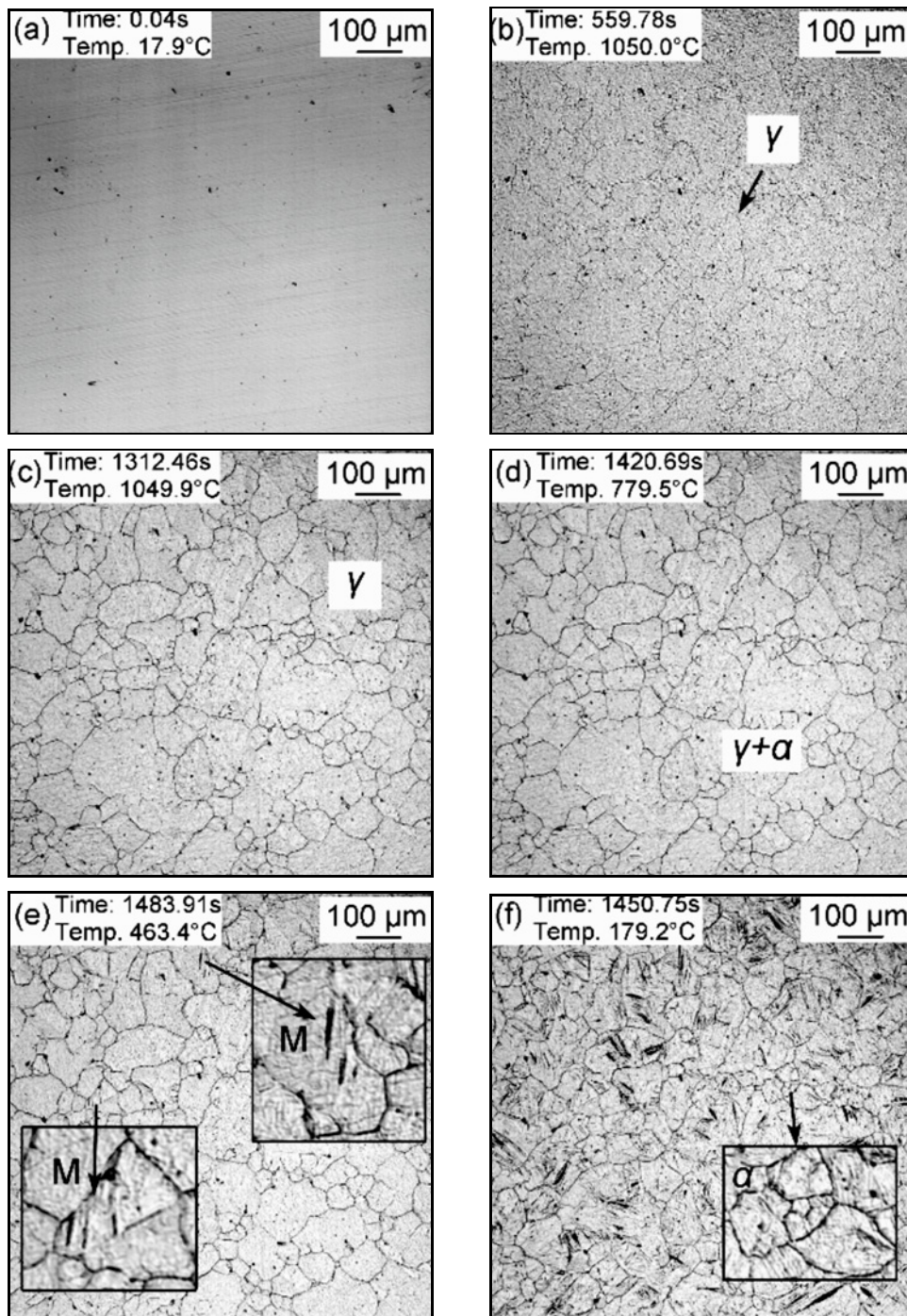


Fig. 2. In-situ observation of microstructure evolution during (a) start heating, (b) austenitization at 1050°C, (c) austenitization for 15 min, (d) critical temperature of 780°C, (e) martensite transformation at 463.4°C, and (f) quenching ending.

loading speed of 1 mm min^{-1} . Besides, the microhardness tests were performed to demonstrate the ferrite and martensite further. Image software Image Pro Plus was used to determine the volume fraction of ferrite and martensite in the quenched specimens. More than three images were analyzed to ensure the accuracy of the measurement. Furthermore, the grain size measurement was determined using the software Nano Measure, using five images and about 100 grains to ob-

tain the grain size distribution in different specimens.

3. Results and discussion

3.1. In-situ observation

Figure 2 displays the transformation during the austenitization and martensite transformation. Only

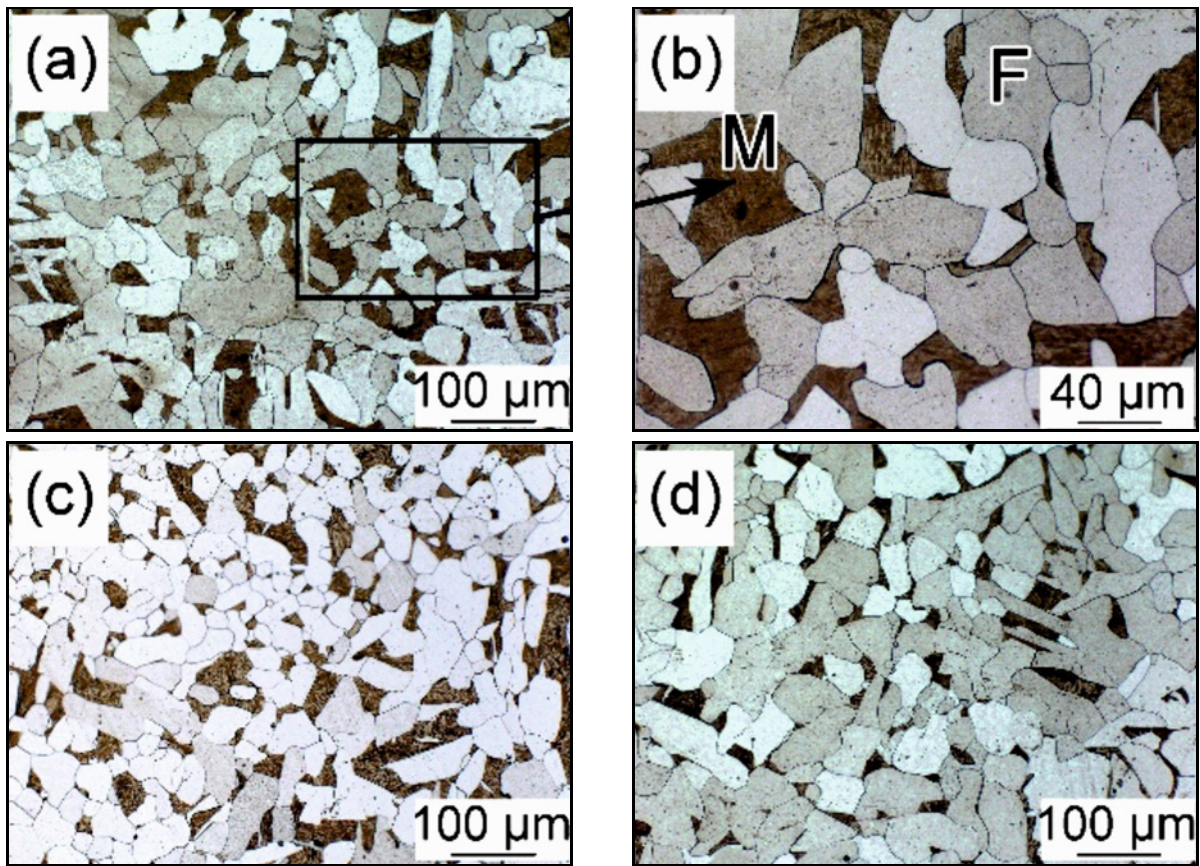


Fig. 3. Morphologies of ferrite and martensite in specimens treated by different holding times of (a) and (b) 3 min, (c) 10 min, and (d) 15 min at 780°C.

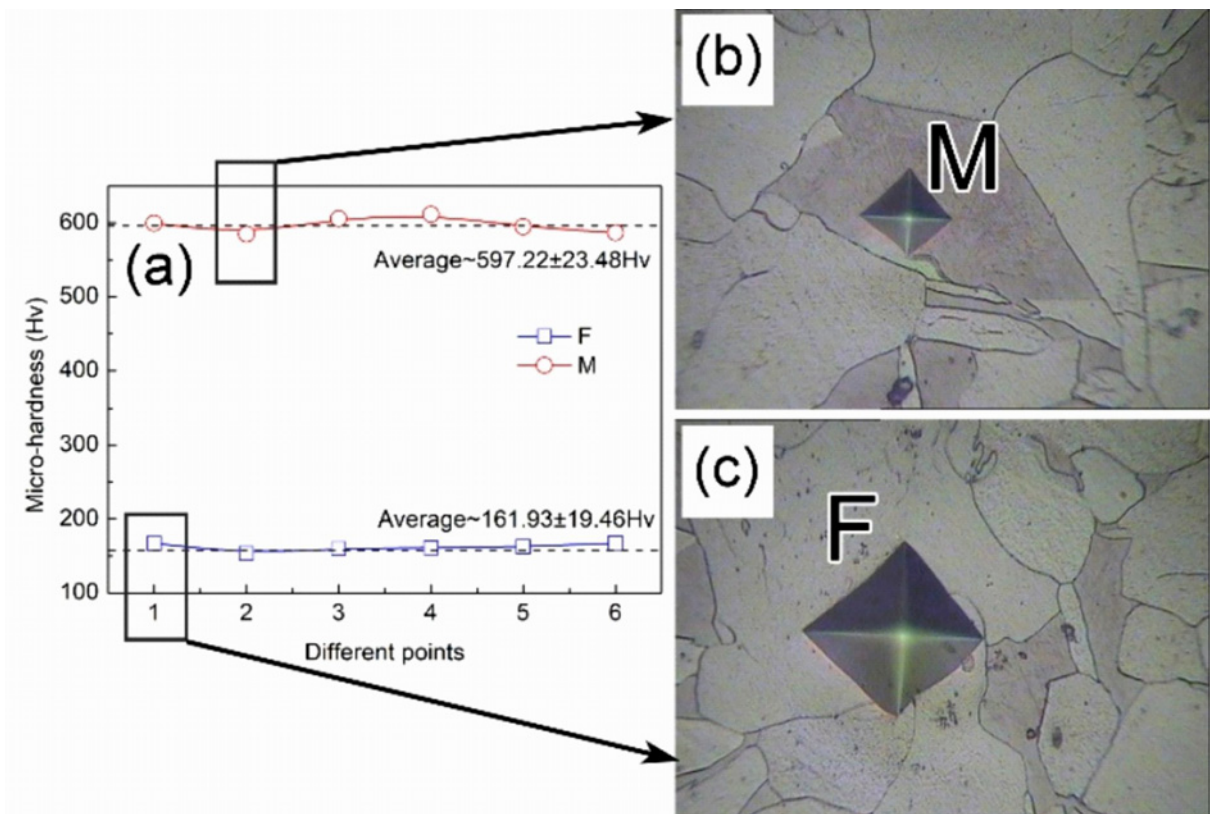


Fig. 4. (a) Microhardness of (b) martensite and (c) ferrite in specimen treated by holding time of 3 min at 780°C.

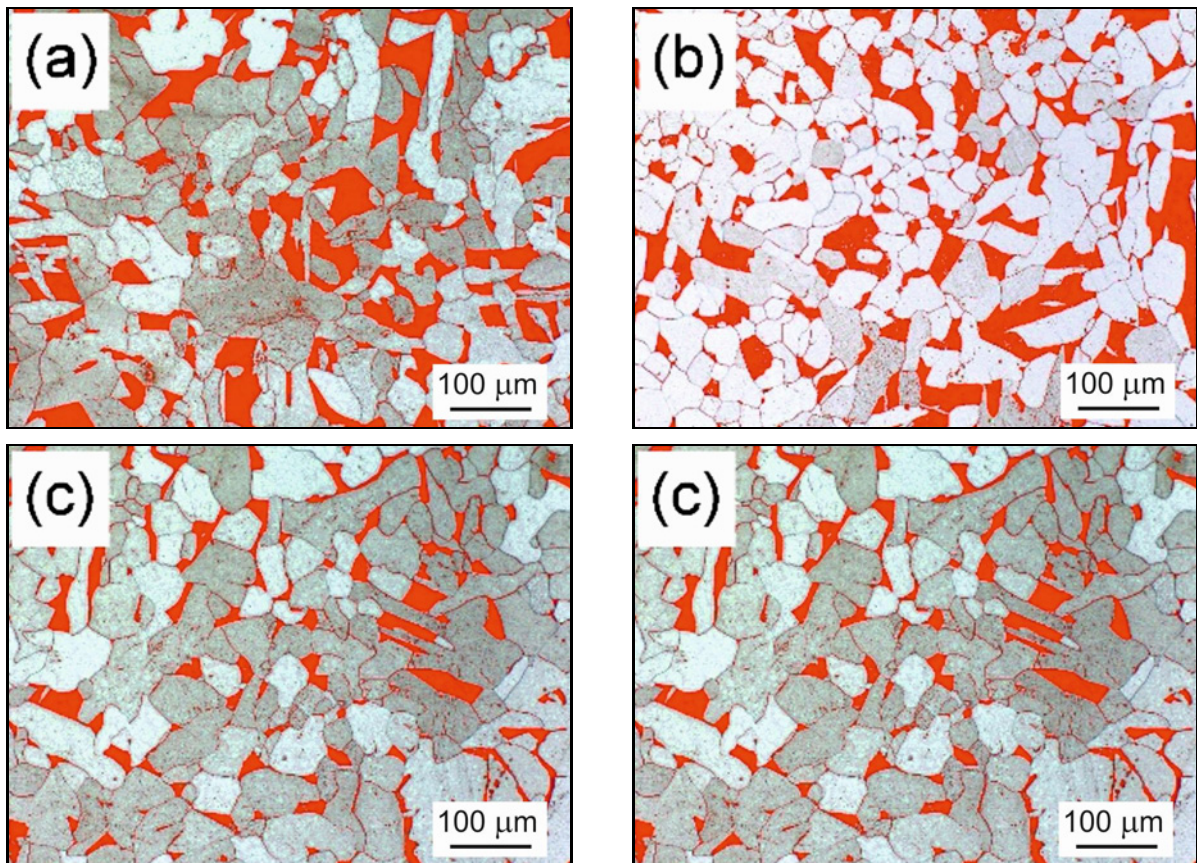


Fig. 5. Volume fractions of ferrite and martensite in three specimens held at (a) 3 min, (b) 10 min, (c) 15 min, and (d) volume fraction results.

dark particles were observed in the room temperature specimen before heating (Fig. 2a). Very apparent austenite grains appeared at 1050°C (Fig. 2b), and the grain boundaries of austenite became more and more clear due to the long-time thermal etching (Fig. 2c). Ferrite transformation was not directly captured at 780 ° by in-situ observation (Fig. 2d) because of same crystalline structure between austenite and ferrite; however, the untransformed grains were confirmed to be the ferrite formed at 780°C because the remaining austenite would transform to martensite during quenching (Fig. 2f). Martensite transformation occurred at 463.4°C during cooling. The martensite laths initiated at the grain boundaries of austenite grains and then extended towards the grains. Ferrite grains formed at 780°C were retained during the quenching. Hence, martensite laths were only found inside partial grains [25–28].

3.2. Microstructure evolutions

Morphologies of the quenched specimens treated by different holding times at a critical temperature of 780°C are presented in Fig. 3. Apparent dual-phase microstructures consisting of polygonal ferrite (light grey) and martensite (dark brown) were observed in

the three specimens. The polygonal ferrite surrounded the martensite. Microhardness results of the specimen held at 780°C for 3 min are given in Fig. 4 to ensure the ferrite and martensite. An obvious smaller rhombic indentation was found in the dark brown phase. The average microhardness of martensite was 597.22 ± 23.48 HV, much larger than that of the ferrite grains (161.93 ± 19.46 HV). It was concluded that the dual-phase ferrite and martensite could be obtained by holding at a critical temperature of 780°C.

Color identification was used in the ferrite and martensite to acquire its volume fraction using *Image-Pro Plus*. The volume fractions of ferrite and martensite in three specimens were determined in Fig. 5. The volume fraction of ferrite (α) increased from 55.8% in 3 min to 65.1% in 10 min, and then 85.3% in 15 min. Correspondingly, the martensite volume fraction (γ) decreased from 44.2% in 3 min to 34.9% in 10 min, then 14.7% in 15 min. That is to say, more ferrite was obtained with the increase of holding time at the critical temperature of 780°C.

All specimens were cold rolled by 50% reduction in thickness after quenching to form distorted ferrite and martensite. The cold rolled ferrite and martensite in different specimens are exhibited in Fig. 6. Very apparent streamline morphology was found along the

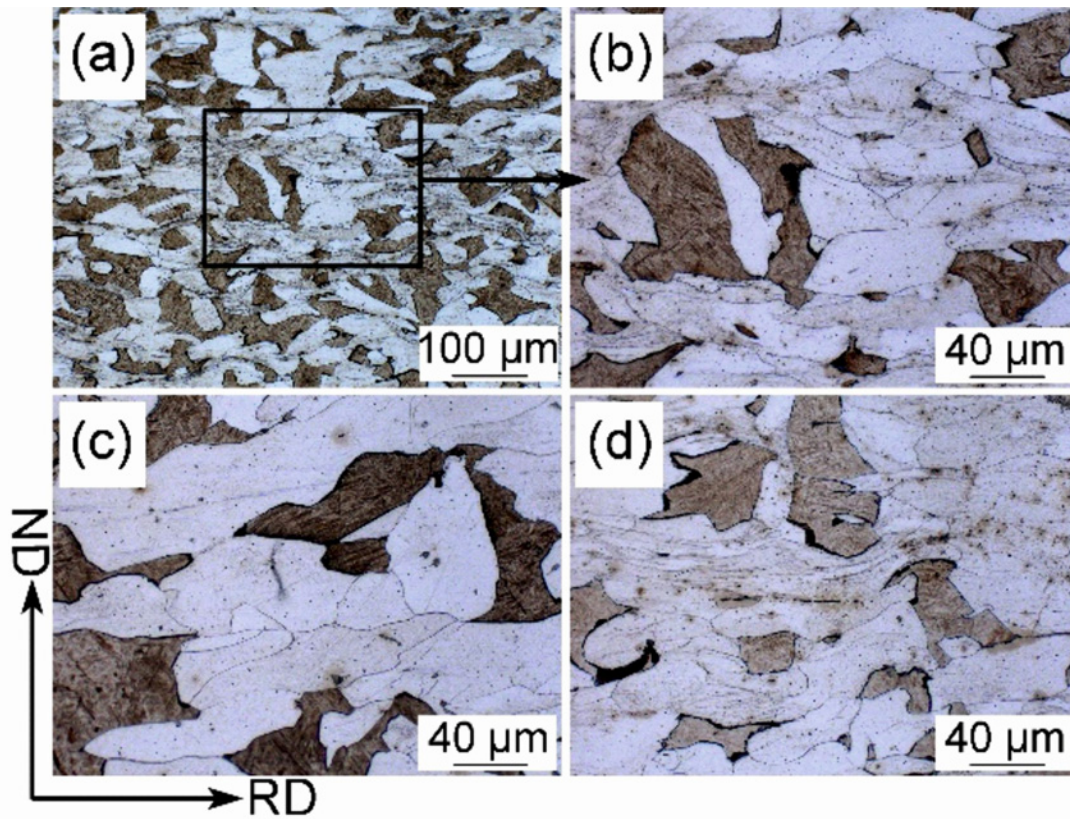


Fig. 6. Morphologies of deformed ferrite and martensite in specimens treated by different holding times of (a) and (b) 3 min, (c) 10 min, and (d) 15 min at 780°C.

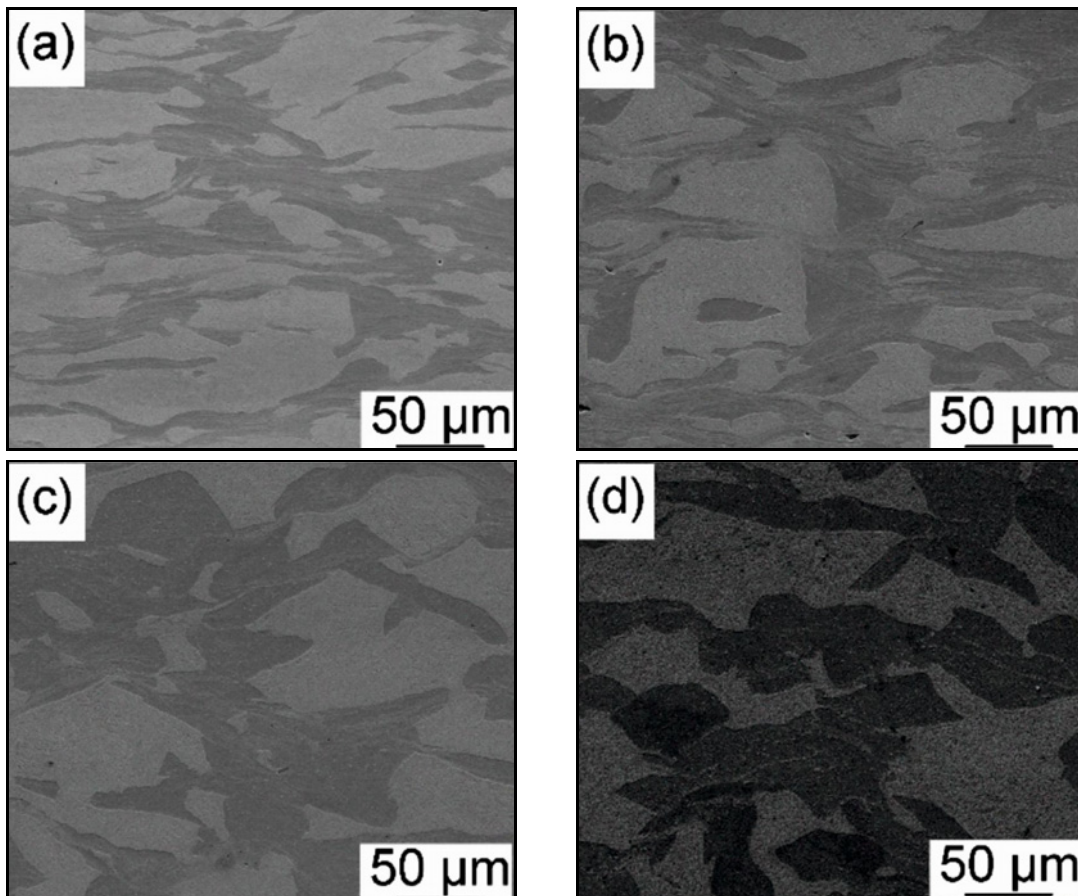


Fig. 7a–d. Morphologies of specimens with increased holding time at 780°C annealed at (a), (b), and (c) 400°C and (d) 450°C.

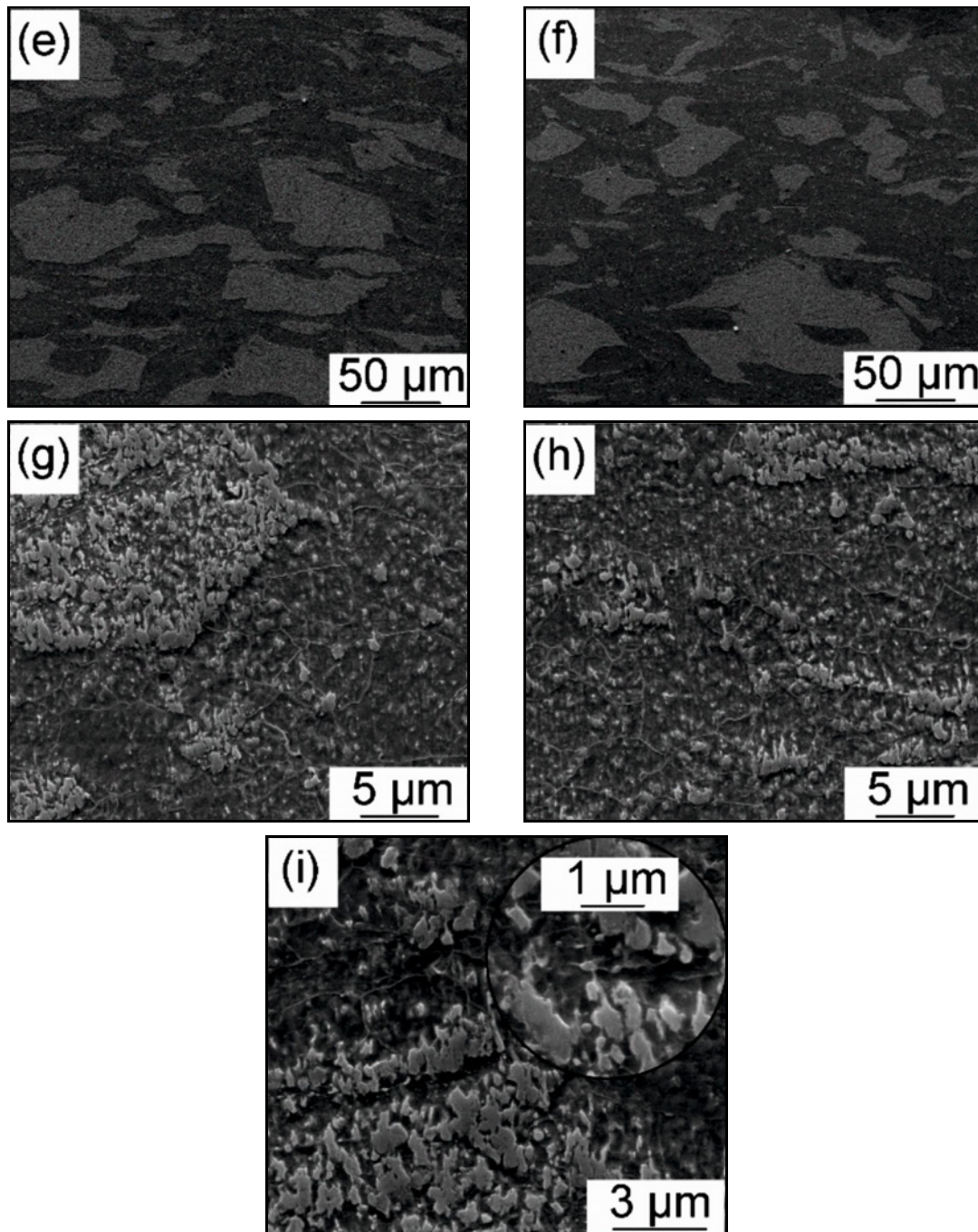


Fig. 7e–i. Morphologies of specimens with increased holding time at 780°C annealed at (e), (f), (g), (h), and (i) 450°C.

rolling direction (RD). However, the deformation degree in ferrite grains was much larger than that in martensite. The deformed ferrite grains were considered the soft phase, which was easily deformed due to their relatively lower microhardness. Meanwhile, the martensite with larger microhardness was hard to deform and inclined to retain its blocky feature.

Morphologies of different specimens annealed at 400°C and 450°C for 30 min are shown in Fig. 7. Streamline morphology of most ferrite and martensite remained in the specimens annealed at 400°C, but

some polygonal ferrite grains with blurry grain boundaries were found. It indicated that almost no static recrystallization happened at 400°C. However, some deformed and recrystallized large-size ferrite grains were easy to find in the specimens annealed at 450°C, and the grain boundaries of ferrite grains became more distinct. Besides, some recrystallized grains were captured within the blocky martensite. The blocky martensite presented the morphology of martensite + recrystallized ferrite grain, manifesting the preliminary static recrystallization at 450°C. In other words,

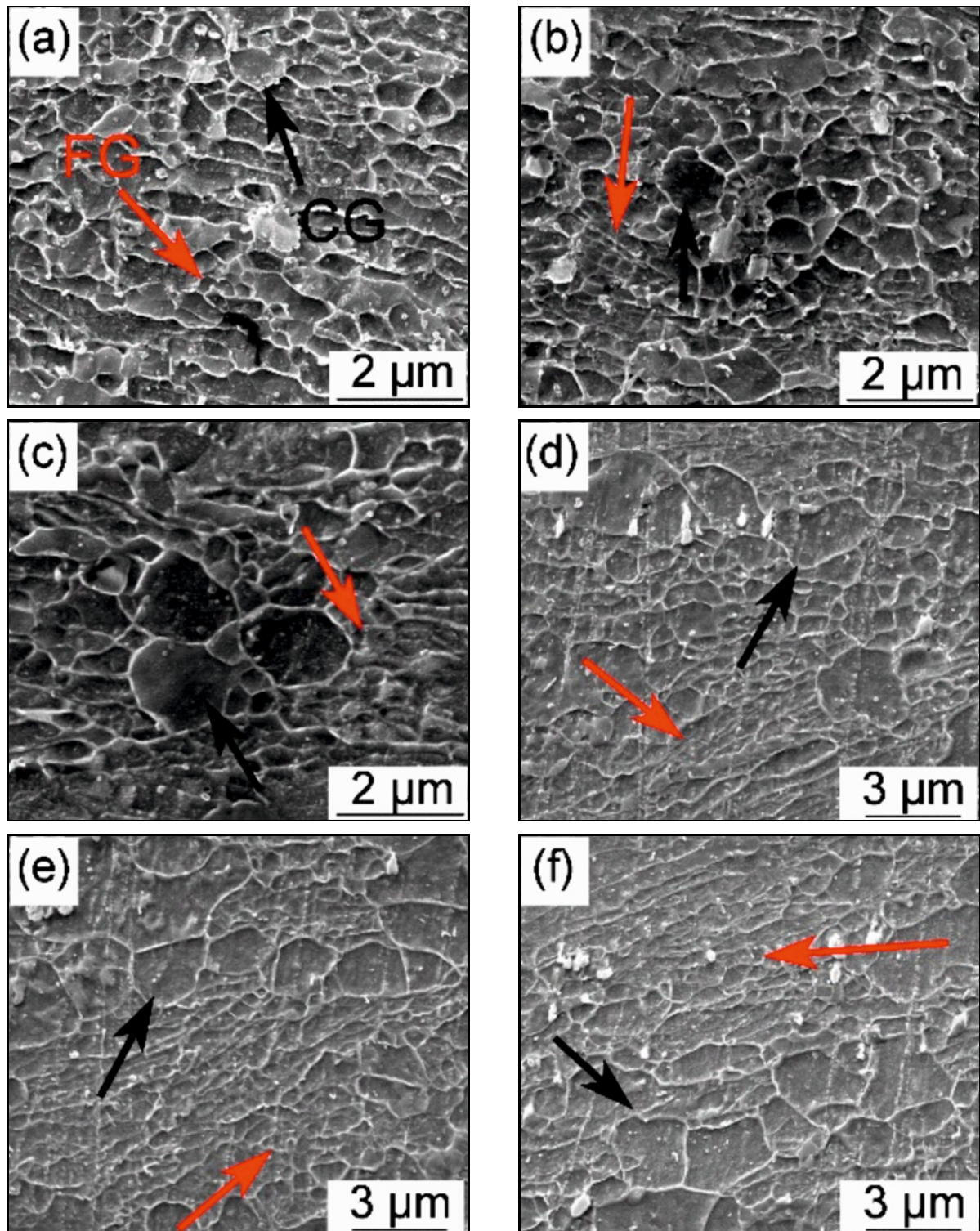


Fig. 8. Morphologies of specimens with increased holding time at 780°C annealed at (a), (b), and (c) 500°C and (d), (e), and (f) 550°C.

static recrystallization was found more in the soft ferrite grains than in deformed martensite. This might be caused by the higher carbon content in martensite and the precipitations that hindered the static recrystallization.

Morphologies of different specimens annealed at 500 and 550°C for 30 min are displayed in Fig. 8. Streamline morphology of deformed ferrite and martensite disappeared. Typical polygonal ferrite grains in bimodal grain size were found throughout the speci-

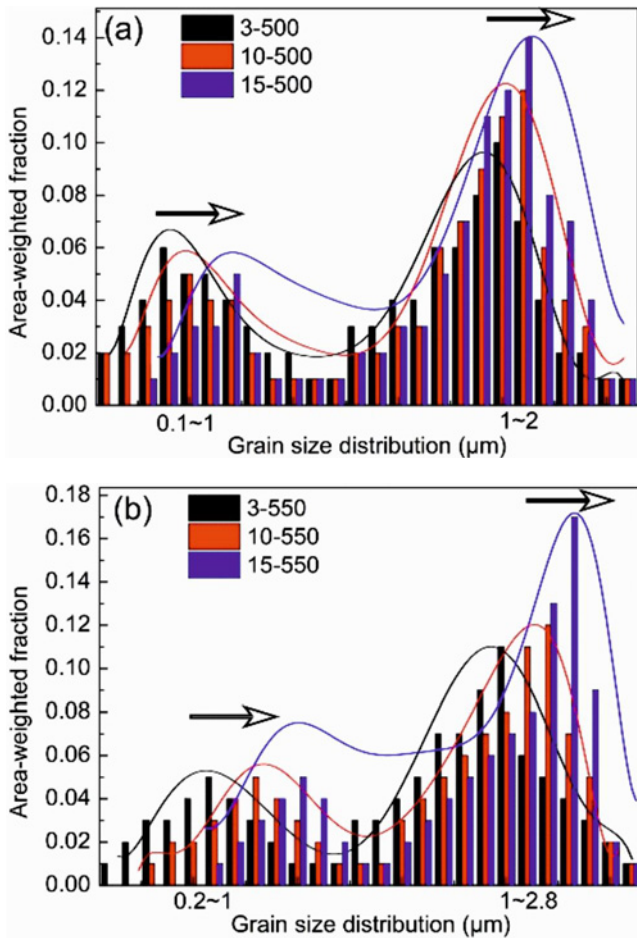


Fig. 9. Grain size distribution of annealed specimens at (a) 500°C and (b) 550°C.

mens. The polygonal ferrite grains demonstrated complete static recrystallization at 500 and 550°C. Then, it can be found that the ferrite grains could be summarized as two types: coarse grains (CG, black arrows) and fine grains (FG, red arrows). According to much existing literature, it could be speculated that the CGs were transformed from the deformed existing ferrite grains, while these FGs occurred by the recrystallization of deformed martensite [21, 22]. It has been proved that the ultrafine ferrite grains were easy to form from the deformed martensite because of the higher distortion energy. The coarse grains were surrounded by many fine grains. With the increase of holding time from 3 to 15 min at 780°C, it can be found the volume fraction of FG decreased apparently. Moreover, some white spherical particles identified as cementite were observed in the matrix.

The grain size distribution of annealed specimens treated by different holding times at 780°C is manifested in Fig. 9. Apparent bimodal grain size was roughly determined according to the grain size smaller or larger than 1 μm. Despite the annealing tempe-

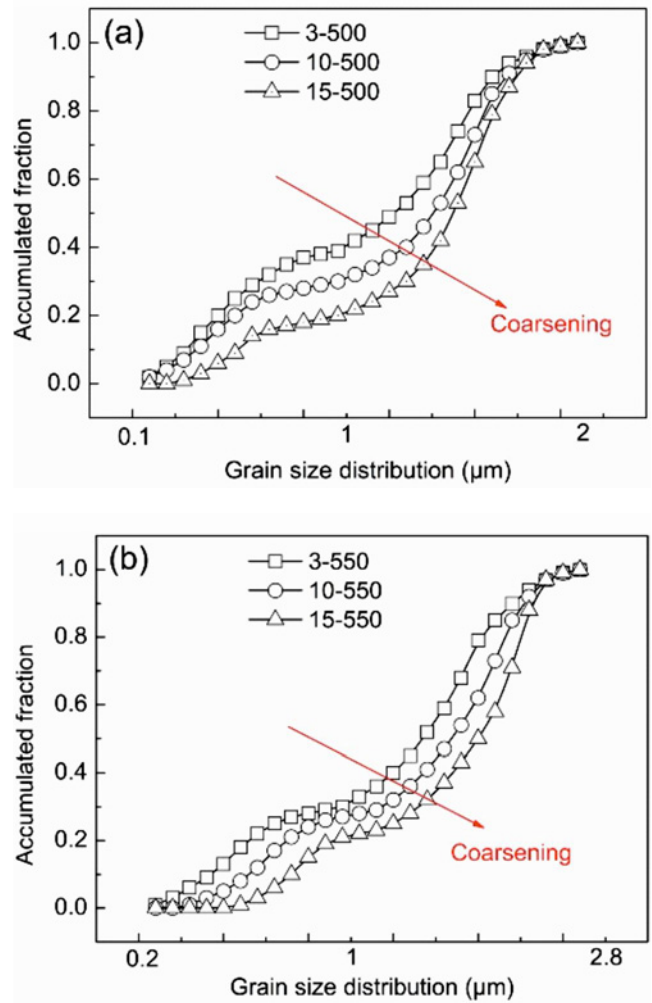


Fig. 10. Accumulated fraction and grain size distribution in annealed specimens at (a) 500°C and (b) 550°C.

ature of 500 and 550°C, the crest moved towards the area of the coarsening grains with the increase of holding time at 780°C. This was because the volume fraction of ferrite in dual-phase ferrite and martensite microstructure increased with the holding time at 780°C, resulting in more coarsening recrystallized ferrite grains during annealing. The reduction of volume fraction in martensite resulted in a decrease in FGs.

Figure 10 displays the relationship between accumulated fraction and grain size distribution in annealed specimens at 500 and 550°C. The “S” curves moved towards the bottom right corner with the increasing holding time at 780°C. It indicated that the average grain size increased with the increase in holding time. Besides, the size distribution of 0.1–2 μm at an annealing temperature of 500°C changed to 0.2–2.8 μm at an annealing temperature of 550°C, signifying the increased average grain size with the increase of annealing temperature.

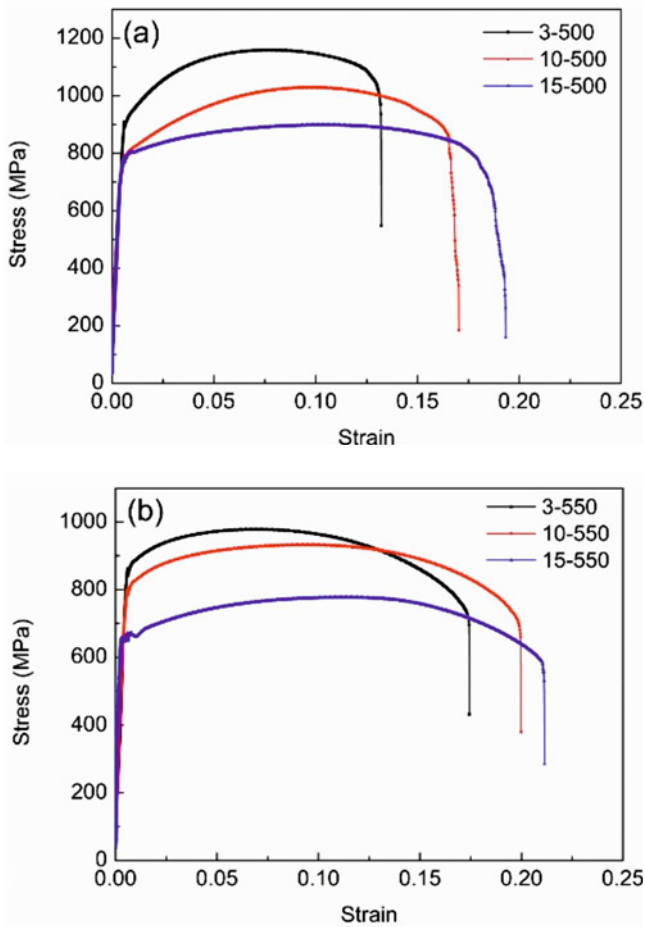


Fig. 11. Mechanical properties of specimens annealed at (a) 500 and (b) 550 °C.

According to the principle of physical metallurgy, the carbon content of subcritical quenched martensite in hypoeutectoid steel was much higher than that of ferrite. After deformation, the recrystallization kinetics of deformed quenched martensite was much slower than that of ferrite. Meanwhile, carbides precipitated from martensite hindered the growth of recrystallized grains. Therefore, the deformed martensite was recrystallized by annealing to form FGs and the original ferrite to produce relatively large ferrite grains. In addition, the smaller recrystallization nucleation rate in the original ferrite contributed to the coarsening CGs. The volume fraction of martensite and ferrite, decided by the fraction of CGs and FGs, was determined by the holding time at the critical temperature. Therefore, the holding time at critical temperature controlled the grain size distribution of bimodal grains.

3.3. Mechanical properties

The mechanical properties of specimens annealed at 500 and 550 °C are displayed in Fig. 11. It was sur-

prising to find that the tensile strength reached about 1159.3 ± 14.87 MPa in specimen 3-500 (holding time-annealing temperature), which was two times more than that for the initial coarse-grained steel. The tensile strength decreased to 1029.4 ± 10.21 MPa (10-500) and 897.74 ± 8.42 MPa (15-500) with the increased elongation of 17.53 ± 1.35 % (10-500) and 19.33 ± 1.40 % (15-500), respectively. In addition, the tensile strength decreased from 979.12 ± 9.61 MPa (3-550) to 933.48 ± 9.22 MPa (10-550) and then 777.04 ± 7.14 MPa (15-550), accompanied by the increased elongation of 17.44 ± 1.35 % (3-550) to 19.98 ± 1.4 % (10-550) and then 21.20 ± 1.43 % (15-550). More importantly, the elongation fluctuated from 13.23 ± 1.22 % to 21.20 ± 1.43 %, indicating a fair ductility and product of strength and elongation (PSE). It should be noted that the strength could be enhanced in most UFGs with a great sacrifice in elongation. However, introducing ferrite before quenching in the martensite and ferrite dual-phase microstructure substantially improved the elongation and the PSE. Meanwhile, the tensile strength could be ensured to be high, two times larger than the coarsen counterparts. The tensile strength in specimens annealed at 500 and 550 °C decreased with the increase of holding time at 780 °C, whereas the ductility increased with the increased holding time. In addition, the tensile strength in specimens annealed at 500 °C was larger than that in specimens annealed at 550 °C with the same holding time at 780 °C.

Figure 12 presents the variation of mechanical properties with the holding time at the critical zone (780 °C) in specimens annealed at 500 and 550 °C. The tensile strength decreased with the increased ferrite percentage, while the elongation increased with the increase of ferrite percentage. The tensile strength reached about 777.04 ± 7.14 MPa at 550 °C and 897.74 ± 8.42 MPa at 500 °C, although the ferrite percentage was 85.3 %. This was because the initial large ferrite grains were cold rolled at room temperature and recrystallized to form newborn, relatively smaller ferrite grains. Besides, it was found that the tensile strength decreased more obviously than elongation with increased ferrite percentage. This might be explained by the further refined grains in UFGs, which showed that the tensile strength was more sensitive to the scale change than the elongation.

3.4. Discussion

Table 1 presents the strength-ductility synergy in different UFG steels. It illustrated that the developed ferrite steels with bimodal grain size distribution exhibited excellent tensile strength and elongation. More importantly, the strength was greatly enhanced without much sacrifice of ductility. Besides, compared to some high-strength UFG steels, the composition of the

Table 1. Summary of the strength-ductility synergy in different UFG steels

Ref.	Chemical composition (wt.%)	TS (MPa)	E (%)	PSE (GPa %)	Mean size
[4]	Fe-0.13C-0.0043N-0.01Si-0.37Mn-0.020P-0.004S	870	20	17.4	180 nm
[21]	Fe-0.17C-0.74Mn-0.04Al-0.008P-0.009S-0.0047N	550	14	7.92	< 2 μm & 3–15 μm
[21]	Fe-0.165C-0.211Si-0.448Mn-0.028Nb-0.013P-0.013S-0.001Als-0.0028N	990.8	15.5	15.36	350 nm
[22]	Fe-0.111C-10.08Ni-0.01Mn-0.001P-0.006Si-0.33Al-0.0017S	820	29	23.78	460 nm
[23]	Fe-0.13C-0.13Si-0.49Mn-0.013P-0.015S	1180/810	9.8/16.8	11.56/13.61	125 nm/650 nm
[29]	Fe-0.165C-0.211Si-0.448Mn-0.014P-0.013S-0.002Als	870	15.5	13.485	330 nm
[30]	Fe-0.165C-0.211Si-0.448Mn-0.014P-0.013S-0.002Als	970.2	12.34	11.97	132 nm
[31]	Fe-0.10C-0.001Si-1.98Mn-0.018Nb-0.0015B-0.002P-0.018Al-0.0011N	966	8.4	8.11	490–850 nm
[32]	Fe-0.12C-0.24Si-1.42Mn-0.012P-0.004S-0.014Nb	788	21.6	17.02	0.7–5.0 μm
[33]	Fe-0.1C-10Cr-5Ni-8Mn	1102	32	35.26	100 nm
[34]	Fe-(0.13–0.17)C-0.4Si-Mn-Cr-(0–0.12)Nb	614–1323	9–19	11.67–11.91	1.4–4.9 μm
[35]	Fe0.13C0.004Ni0.37Mn0.020P0.004S0.043Als	870	20	17.4	180 nm
[36]	Fe-0.10C-0.40Mn-0.23Si-0.14Cr-0.025P-0.005S	532	21	11.17	1 μm

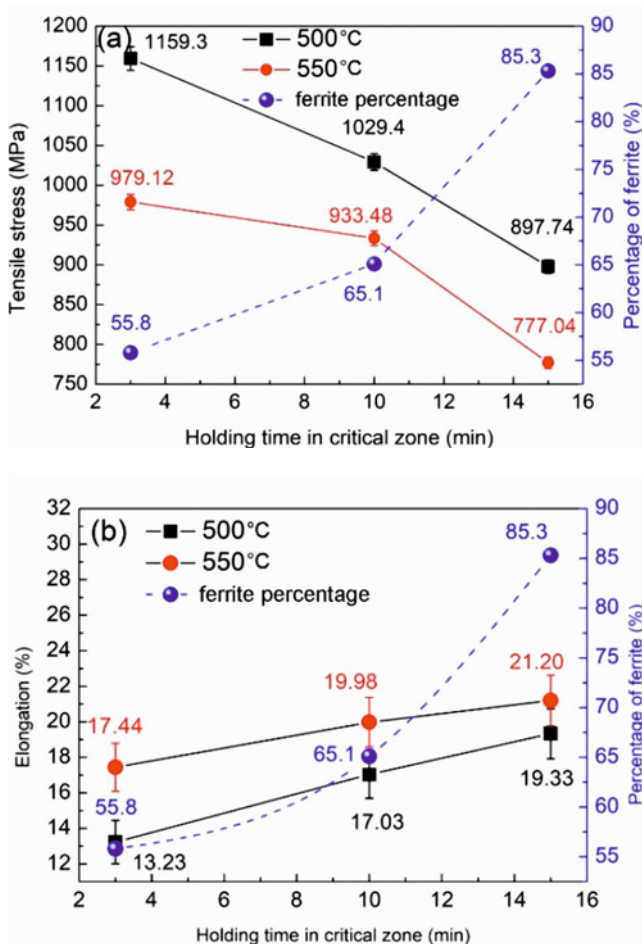


Fig. 12. Variation of (a) tensile strength and (b) elongation with the holding time at 780°C in annealed specimens.

studied ferrite steels with bimodal grain size distribution was very simple. No costly alloy elements were added to the ferrite steels with bimodal grain size distribution. Furthermore, the fabrication of ferrite steels

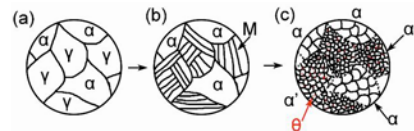


Fig. 13. Microstructure evolution of ferrite grain with bimodal size.

with bimodal grain size distribution was normal without severe plastic deformation, like cold rolling of fully martensite or bainite initial microstructure.

The microstructure evolution of ferrite grain with bimodal size is exhibited in Fig. 13. The introduction of ferrite grain at the critical temperature of 780°C was the key process to result in the CGs. The combination of strength and plasticity was affected by the volume fraction of fine and coarsening ferrite grains. The range of volume fractions of different grain sizes in bimodal size was based on the volume fractions of ferrite and martensite in the primary dual-phase microstructure. The more martensite in the primary dual-phase microstructure, the larger the number of fine grains and the smaller the number of coarse grains. In addition, the cementite particles precipitated around the primary martensite laths also contributed to enhanced strength and elongation. According to the abovementioned results, the ferrite percentage dominated the mechanical properties and was controlled by the holding time at critical temperatures. Therefore, it was possible to achieve a hierarchical design in the bimodal grains of UFGs via ratio regulation on the dual-phase ferrite/martensite.

The morphology of ferrite grains after deformation was discovered in Fig. 14. It revealed that more dislocation lines were captured in the coarse ferrite grains, while very few dislocation lines were found in the fine grains. The accumulated dislocation lines in the coarse grains were attributed to the relatively large size to accommodate the dislocations. More importantly, the

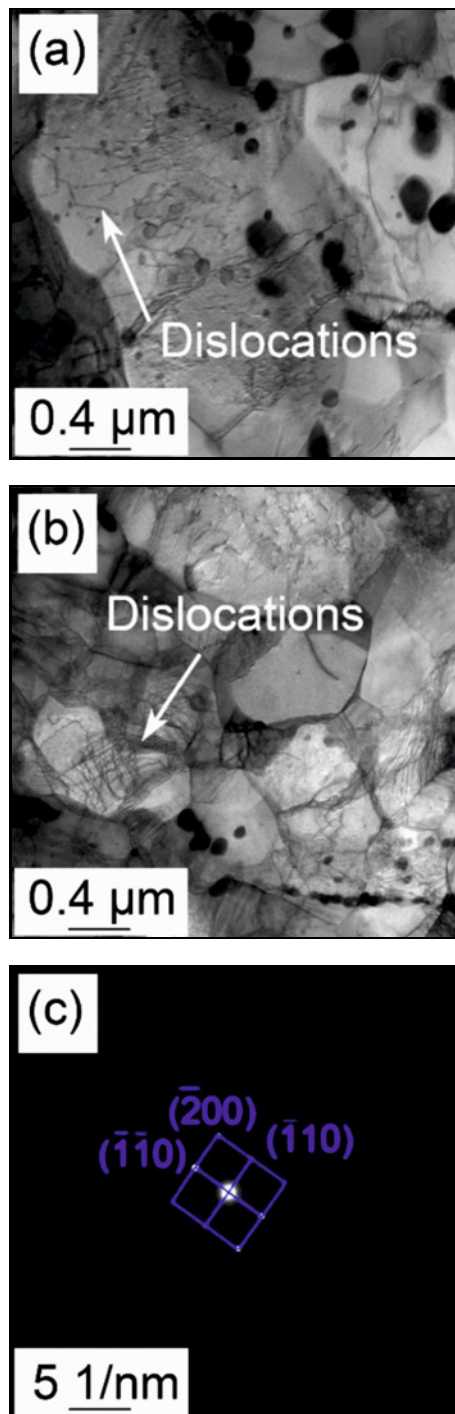


Fig. 14. (a) and (b) The accumulated dislocations in coarse ferrite grains and (c) corresponding selected area diffraction of ferrite grains.

relatively soft coarse grains were easy to deform and then caused the Geometrically Necessary Dislocations (GNDs). In polycrystalline materials, when tensile deformation occurs, slip transfers from grains that undergo plastic deformation to adjacent grains. Whether this transfer can occur mainly depends on whether the stress concentration generated by the dislocation

pile-up near the grain boundary of the already slipped grain can activate the dislocation sources in the slip systems of adjacent grains, causing them to initiate and engage in coordinated multiple slips. Large grains exhibit greater stress concentration due to the larger distance from the grain boundary to the dislocation source and a larger number of dislocations. This results in large grains initiating plastic deformation in adjacent grains under relatively small applied stresses. In contrast, small grains have a smaller distance from the grain boundary to the dislocation source and fewer dislocations, leading to smaller stress concentration. Therefore, larger applied stresses are required to induce plastic deformation in adjacent grains. Grain boundaries play a crucial role in stress transfer in polycrystalline materials. During tensile deformation, stress is transmitted from one large grain to adjacent small grains through grain boundaries. During this process, dislocations continuously proliferate within grains and cross grain boundaries to adjacent grains. This transfer and accumulation of dislocations lead to plastic deformation of grains and stress redistribution [21, 32].

The enhanced tensile strength could be attributed to the refined ferrite grains, which provided a better grain refinement effect. Besides, the precipitated cementite particles from the supersaturated martensite offered a precipitation effect. The deformation of coarsening grains in the bimodal distribution microstructure was bound to be confined by the surrounding hard fine grains under external load. Therefore, the uneven strain distribution occurred within the coarsening grains [37]. The deformation limitation was greatest since the grain boundary of the coarsening grains was in direct contact with the fine grains. Thus, a significant plastic strain gradient was formed along the radius towards the coarsening grains.

Dislocations occurred simultaneously in both the coarse and fine grains during the deformation process of the soft coarsening and hard fine grains. The dislocations were more likely to move in the coarsening grains than in the fine grains because the larger grain had less resistance to slip. The fine grains bearded more stress because of the load transfer, and only a small amount of the load was transferred to the coarsening grains. The larger the volume fraction of the coarsening grains, the greater the load that can be transferred. In addition, the stress concentration in the fine grains was released due to load transfer, which reduced the possibility of plastic instability. Plastic flow was generated in the soft coarsening grains, which improved the plasticity of the bimodal distribution structure. The plastic strain gradient in the coarsening grains was only related to the geometrical characteristics of the coarsening grains. The average plastic strain gradient increased when the size of coarsening grains decreased, and then the accumu-

lation of additional geometric necessary dislocation to coordinate the non-uniform strain in the coarsening grains increased. In the initial stage of tensile deformation, the stress changes linearly with strain, and the material undergoes elastic deformation at this point. The stress distribution between large and small grains is relatively uniform during this stage. As the strain increases, the material enters the plastic deformation stage. At this stage, due to the larger stress concentration in large grains, they undergo plastic deformation preferentially and transmit stress to adjacent small grains. The small grains will also undergo plastic deformation under stress, but the degree of deformation is relatively small. Consequently, the bimodal distribution microstructure achieved a higher deformation ability [37].

The combination of strength and ductility could be designed by the ratio regulation on the dual-phase ferrite/martensite. The most valuable technical was the holding time at critical temperature to obtain different ferrite volume fractions. The holding time affected the volume fraction of ferrite and changed the size distribution of ferrite grains, which dominated the final mechanical properties. Furthermore, the annealing temperature also influenced the size distribution of ferrite grains.

4. Conclusions

(1) Ferrite grains with bimodal distribution were obtained by thermal holding at a critical temperature of 780 °C and subsequent cold rolling and annealing. The more martensite in the primary dual-phase microstructure, the larger the number of fine grains and the smaller the amount of coarse grains. Thus, hierarchical design in the bimodal grains of UFGs via ratio regulation on the dual-phase ferrite/martensite could be achieved by the holding time.

(2) The tensile strength decreased with the increased holding time at critical temperature, while the elongation increased with the increasing holding time. The volume fraction of introduced ferrite and the final grain size distribution of ferrite affected the comprehensive mechanical properties.

(3) The elongation was ensured by the better work hardening ability in coarsening grains and plastic strain gradient between ferrite grains with a bimodal distribution.

Acknowledgements

The authors gratefully acknowledge the financial support from the Competitive Scientific and Technological Research Projects of Quzhou Science and Technology Bureau (2024K180) and Guiding Scientific and Technological Research Projects of Quzhou Science and Technology Bureau (Y202455648).

References

- [1] R. Zhang, W. Q. Cao, Z. J. Peng, J. Shi, H. Dong, C. H. Huang, Intercritical rolling induced ultrafine microstructure and excellent mechanical properties of the medium-Mn steel, *Mater. Sci. Eng. A* 583 (2013) 84–88. <http://dx.doi.org/10.1016/j.msea.2013.06.067>
- [2] K. Lu, Making strong nanomaterials ductile with gradients, *Science* 345 (2014) 1455–1456. <https://doi.org/10.1126/science.1255940>
- [3] B. F. Wang, J. Y. Sun, J. D. Zou, S. Vincent, J. Li, Mechanical responses, texture and microstructural evolution of high purity aluminum deformed by equal channel angular pressing, *J. Cent. South Univ.* 22 (2015) 3698–3074. <https://doi.org/10.1007/s11771-015-2912-0>
- [4] N. Tsuji, R. Ueji, Y. Minamino, Y. Saito, A new and simple process to obtain nano-structured bulk low-carbon steel with superior mechanical property, *Scripta Mater.* 46 (2002) 305–310. [https://doi.org/10.1016/S1359-6462\(01\)01243-X](https://doi.org/10.1016/S1359-6462(01)01243-X)
- [5] R. Ueji, N. Tsuji, Y. Minamino, Y. Koizumi, Ultra-grain refinement of plain low carbon steel by cold rolling and annealing of martensite, *Acta Mater.* 50 (2002) 4177–4189. [https://doi.org/10.1016/S1359-6454\(02\)00260-4](https://doi.org/10.1016/S1359-6454(02)00260-4)
- [6] K. Matsybara, Y. Miyahara, Z. Horita, T. G. Langdon, Developing superplasticity in a magnesium alloy through a combination of extrusion and ECAP, *Acta Mater.* 51 (2003) 3073–3084. [https://doi.org/10.1016/S1359-6454\(03\)00118-6](https://doi.org/10.1016/S1359-6454(03)00118-6)
- [7] D. H. Shin, B. C. Kim, K. Park, Y. S. Kim, Microstructure evolution in commercial low carbon steel by equal channel angular pressing, *Acta Mater.* 48 (2000) 2247–2255. [https://doi.org/10.1016/S1359-6454\(00\)00028-8](https://doi.org/10.1016/S1359-6454(00)00028-8)
- [8] R. Z. Valiev, Y. Ivanisenko, E. F. Rauch, B. Baudelet, Microstructural evolution and the mechanical properties of an aluminum alloy processed by high-pressure torsion, *J. Mater. Sci.* 47 (2012) 7789–7795. <http://dx.doi.org/10.1007/s10853-012-6524-x>
- [9] P. J. Hurley, P. D. Hodgson, Effect of process variables on the formation of dynamic strain induced ultrafine ferrite during hot torsion testing, *Mater. Sci. Tech.* 17 (2001) 1360–1368. <https://doi.org/10.1179/026708301101509566>
- [10] Y. Saito, H. Utsunomiya, N. Tsuji, T. Sakai, Novel ultra-high straining process for bulk materials – development of the accumulative roll-bonding (ARB) process, *Acta Mater.* 47 (1999) 579–583. [https://doi.org/10.1016/S1359-6454\(98\)00365-6](https://doi.org/10.1016/S1359-6454(98)00365-6)
- [11] N. Tsuji, K. Shiotsuki, Y. Saito, Super plasticity of ultra-fine grained Al-Mg alloy produced by accumulative roll-bonding, *Mater. Trans. JIM* 40 (1999) 765–771. <https://doi.org/10.2320/matertrans1989.40.765>
- [12] Q. X. Zhang, Q. Yuan, Z. T. Wang, W. W. Qiao, G. Xu, Enhanced mechanical properties in a low-carbon ultrafine grain steel by niobium addition, *Metall. Mater. Trans. A* 52 (2021) 5123–5132. <https://doi.org/10.1007/s11661-021-06459-3>
- [13] Q. X. Zhang, Q. Yuan, Z. T. Wang, W. W. Qiao, G. Xu, Enhanced thermal stability of the low-carbon ultrafine grain steel with nanoprecipitates, *Steel Res.*

- Int. 93 (2022) 2100320.
<https://doi.org/10.1002/srin.202100320>
- [14] K. Lu, Gradient nanostructured materials, *Acta Metallurgica Sinica* 51 (2015) 1–10.
<http://dx.doi.org/10.11900/0412.1961.2014.00395>
- [15] H. Azizi, H. S. Zurob, D. Embury, X. Wang, K. Wang, B. Bose, Using architected materials to control localized shear fracture, *Acta Mater.* 143 (2018) 298–305. <https://doi.org/10.1016/j.actamat.2017.10.027>
- [16] X. H. Chen, J. Lu, L. Lu, K. Lu, Tensile properties of a nanocrystalline 316L austenitic stainless steel, *Scripta Mater.* 52 (2005) 1039–1044.
<https://doi.org/10.1016/j.scriptamat.2005.01.023>
- [17] T. Roland, D. Rehrant, K. Lu, J. Lu, Fatigue life improvement through surface nanostructuring of stainless steel by means of surface mechanical attrition treatment, *Scripta Mater.* 52 (2005) 1949–1954.
<https://doi.org/10.1016/j.scriptamat.2006.01.049>
- [18] T. H. Fang, W. L. Li, N. R. Tao, K. Lu, Revealing extraordinary intrinsic tensile plasticity in gradient nano-grained copper, *Science* 331 (2011) 1587–1590.
<https://doi.org/10.1126/science.1200177>
- [19] J. P. Masse, B. Chéhab, H. Zurob, D. Embury, X. Wang, O. Bouaziz, An original way for producing a 2.4 GPa strength ductile steel by rolling of martensite, *ISIJ International* 54 (2014) 235–239.
<https://doi.org/10.2355/isijinternational.54.235>
- [20] Z. T. Wang, Q. Yuan, Q. X. Zhang, S. Liu, G. Xu, Microstructure and mechanical properties of a cold rolled gradient medium-carbon martensitic steel, *Acta Metallurgica Sinica* 59 (2023) 821–828.
<https://doi.org/10.11900/0412.1961.2021.00233>
- [21] H. Azizi-Alizamini, M. Militzer, W. J. Poole, A novel technique for developing bimodal grain size distributions in low carbon steels, *Scripta Mater.* 57 (2007) 1065–1068.
<https://doi.org/10.1016/j.scriptamat.2007.08.035>
- [22] T. S. Wang, F. C. Zhang, M. Zhang, B. Lv, A novel process to obtain ultrafine-grained low carbon steel with bimodal grain size distribution for potentially improving ductility, *Mater. Sci. Eng. A* 485 (2008) 456–460. <https://doi.org/10.1016/j.msea.2007.09.026>
- [23] S. M. Hosseini, M. Alishahi, A. Najafzadeh, A. Kermanpur, The improvement of ductility in nano/ultrafine grained low carbon steels via high temperature short time annealing, *Mater. Lett.* 74 (2012) 206–208.
<http://dx.doi.org/10.1016%2Fj.matlet.2012.01.092>
- [24] Q. Yuan, Z. B. Li, Q. X. Zhang, G. Xu, Towards excellent strength-ductility synergy via high temperature short time annealing in low-carbon ultrafine grain steel, *Mater. Sci. Eng. A* 886 (2023) 145674.
<https://doi.org/10.1016/j.msea.2023.145674>
- [25] Q. Yuan, J. Ren, J. X. Mo, Z. C. Zhang, E. Tang, G. Xu, Z. L. Xue, Effects of rapid heating on the phase transformation and grain refinement of a low-carbon microalloyed steel, *J. Mater. Res. Technol.* 23 (2023) 3756–3771.
<https://doi.org/10.1016/j.jmrt.2023.02.018>
- [26] Q. Yuan, J. Ren, E. Tang, Z. B. Li, J. X. Mo, S. Y. Zhao, G. Xu, Rapid annealing of an ultralow carbon steel: in-depth exploration of the microstructure-mechanical properties evolution, *J. Mater. Res. Technol.* 27 (2023) 1097–1113.
<https://doi.org/10.1016/j.jmrt.2023.09.286>
- [27] Z. B. Li, Q. Yuan, S. P. Xu, Y. Zhou, S. Liu, G. Xu, In situ observation of the grain growth behavior and martensitic transformation of supercooled austenite in NM500 wear-resistant steel at different quenching temperature, *Materials* 16 (2023) 3840–3857. <https://doi.org/10.3390/ma16103840>
- [28] Q. Yuan, J. X. Mo, J. Ren, W. Liang, G. Xu, A detailed exploration of microstructure evolution in a novel Ti-Mo martensitic steel through in-situ observation: The effect of heating rate, *J. Mater. Res. Technol.* 31 (2024) 264–275.
<https://doi.org/10.1016/j.jmrt.2024.06.080>
- [29] Q. Yuan, G. Xu, J. J. Tian, W. C. Liang, The recrystallization behavior in ultrafine-grained structure steel fabricated by cold rolling and annealing, *Arab. J. Sci. Eng.* 42 (2017) 4771–4777.
<https://doi.org/10.1007/s13369-017-2633-9>
- [30] Q. Yuan, G. Xu, M. Liu, M. Liu, H. J. Hu, Evaluation of mechanical properties and microstructures of ultrafine grain low-carbon steel processed by cryorolling and annealing, *Trans. Indian Inst. Met.* 72 (2019) 741–749. <https://doi.org/10.1007/s12666-018-1526-2>
- [31] Y. Okitsu, N. Takata, N. Tsuji, A new route to fabricate ultrafine-grained structures in carbon steels without severe plastic deformation, *Scripta Mater.* 60 (2009) 76–79.
<https://doi.org/10.1016/j.scriptamat.2008.09.002>
- [32] T. S. Wang, Z. Li, B. Zhang, X. J. Zhang, J. M. Deng, F. C. Zhang, High tensile ductility and high strength in ultrafine-grained low-carbon steel, *Mater. Sci. Eng. A* 527 (2010) 2798–2801.
<https://doi.org/10.1016/j.msea.2010.01.072>
- [33] M. Hamzeh, A. Kermanpur, A. Najafzadeh, Fabrication of the ultrafine-grained ferrite with good resistance to grain growth and evaluation of its tensile properties, *Mater. Sci. Eng. A* 593 (2014) 24–30.
<https://doi.org/10.1016/j.msea.2013.09.026>
- [34] A. G. Kalashami, A. Kermanpur, E. Ghassemali, A. Najafzadeh, Y. Mazaheri, Correlation of microstructure and strain hardening behavior in the ultrafine-grained Nb-bearing dual phase steels, *Mater. Sci. Eng. A* 678 (2016) 215–226.
<https://doi.org/10.1016/j.msea.2016.09.108>
- [35] R. Ueji, N. Tsuji, Y. Minamino, Y. Koizumi, Effect of rolling reduction on ultrafine grained structure and mechanical properties of low-carbon steel thermomechanically processed from martensite starting structure, *Sci. Technol. Adv. Mat.* 5 (2004) 153–162.
<https://doi.org/10.1016/j.stam.2003.10.017>
- [36] J. J. Sun, C. Yang, S. W. Guo, X. J. Sun, M. Y. Ma, S. D. Zhao, Y. N. Liu, A novel process to obtain lamella structured low-carbon steel with bimodal grain size distribution for potentially improving mechanical property, *Mater. Sci. Eng. A* 785 (2020) 139339. <https://doi.org/10.1016/j.msea.2020.139339>
- [37] W. Lei, T. S. Wang, Z. Li, X. J. Zhang, Q. F. Wang, F. C. Zhang, A new process to fabricate ultrafine-grained low-carbon steel with high strength and high elongation, *Mater. Sci. Eng. A* 528 (2010) 784–787.
<https://doi.org/10.1016/j.msea.2010.09.072>